



MINISTRY OF TECHNOLOGY

AERONAUTICAL RESEARCH COUNCIL

CURRENT PAPERS

Free-Flight Tests in the Npl 6-in. (15-CM)

Shock Tunnel of Model HB - 2

Using Multiple Spark Recording

By

L. Pennelegion, R. F. Cash and M. J. Shilling

LONDON: HER MAJESTY'S STATIONERY OFFICE

1967

SIX SHILLINGS NET

October, 1966

Free-Flight Tests in the NPL 6-in. (15-cm) Shock Tunnel
of Model HB-2 using Multiple Spark Recording

- By -

L. Pennelegion, R. F. Cash and M. J. Shilling

SUMMARY

Free-flight measurements of axial force, normal force and pitching moment of an HB-2 model have been made in the NPL 6-in. (15-cm) shock tunnel and the results compared with force balance data obtained elsewhere. The displacement of the polyurethane models was recorded as a set of overlapping images on one photographic plate.

CONTENTS/

* Replaces NPL Aero Report 1212 - A.R.C.28 415.

CONTENTS

1. Introduction
 2. Model Construction and Suspension
 3. Test Environment and Model Motion
 4. NPL Photographic Technique
 5. Calculation of Aerodynamic Forces
 6. Discussion of Results
 - 6.1 The flow establishment about the model
 - 6.2 Total axial-force coefficient
 - 6.3 Normal-force coefficient
 - 6.4 Ratio of normal force to axial force
 - 6.5 Pitching-moment coefficient
 7. Conclusions
 8. Acknowledgements
- References
-

List of Symbols

A_t	total axial force	
C_{A_t}	total axial-force coefficient	$\frac{A_t}{q_\infty S}$
C_m	pitching-moment coefficient	$\frac{M}{q_\infty S d}$
C_N	normal-force coefficient	$\frac{N}{q_\infty S}$
N	normal force	
P	reservoir pressure as defined by Wilson and Regan ⁵	
d	reference centrebody diameter	
ℓ	overall length ($4.90 d$)	
M_s	shock-wave Mach number	
M_∞	freestream Mach number	

S	reference area of model $\left(\frac{\pi d^2}{4} \right)$
S ₁	cross-sectional area of sphere
q _∞	freestream dynamic pressure
Re _d	Reynolds number based on centrebody diameter
x	distance along body axis from nose
x _{cp}	distance of centre of pressure from nose
y	distance perpendicular to the body axis
α	angle of attack, deg.
w	weight of free-flight model

1. Introduction

Photographic measurements of the aerodynamic behaviour of freely-flying models in hypersonic wind tunnels were initiated by Geiger¹ at General Electric, Philadelphia, Pa. This early successful work was done in a combustion shock-tunnel facility and used a high-speed framing camera to record the motion of the model. Subsequent developments of the free-flight technique in both short and long duration tunnels have still used framing cameras for recording the motion of the model. A method is used at N.P.L. which eliminates the tedium of successive frame analysis by recording successive images onto one photographic plate by the use of multiple sparks. This provides greater measuring accuracy and more rapid assessment of the model rotation and displacement. Tests were made previously at N.P.L. of the comparative measuring accuracy of the N.P.L. method and of a framing camera using an HB-1 model². The method is only suitable for static derivatives since it is not possible to record sufficient information for oscillatory phenomena. This paper shows the results of tests in the NPL 6-in. (15-cm) shock tunnel on an HB-2 model at M_∞ = 8.6 for initial incidences of -12°, -6°, 0°, 6° and 12°.

2. Model Construction and Suspension

A steel model of the HB-2 was used in a slip-casting technique to produce several moulds having the required internal surface finish and dimensional accuracy. Using Clocel (a closed-cell foamed polyurethane), models were cast in the moulds and extracted when cool. The weight at this stage was approximately 20 gm for a model of diameter 1.46 in. (3.7 cm) and length 7.15 in. (18.2 cm). The centre of the model was successively drilled out, leaving a wall thickness of approximately $\frac{1}{8}$ in. (0.3 cm). A simple

balancing/

balancing jig enabled the centroid to be measured, and counterbalance weights (of order 1 gm) inserted to move the centroid on to the expected centre of pressure. The base of the model was closed by a thin Mylar disc. The disc was stuck on with Durafix and a pinhole placed through it to allow equilibration of pressure during the lengthy preliminary test-section evacuation phase. The total weight at the final stage was approximately 13 gm. Two 10-strand 15 denier nylon threads were nipped into short pieces of hypodermic tubing which were glued into the parallel portion of the body of the model. All but two of the strands were severed at the model on each thread. The required initial incidence was adjusted by a small lever on the support plate under the pitot tube. These mechanical details can be seen in Fig. 2.

3. Test Environment and Model Motion

The technique was developed and all the measurements made in the NPL 6 in. (15 cm) shock tunnel. (Fig. 1.)

The test section of the tunnel has a 16 in. (41 cm) diameter closed-jet following an 11° total angle conical nozzle. The flow Mach number, M_∞ , for the tests was 8.6 with a centreline Mach number gradient of 0.01 per in. (0.004 per cm) and a model Reynolds number, based on model diameter, of 1.83×10^5 .

For these tests the shock tunnel was driven with pure helium at 3000 psi (200 atm) at ambient temperature. The driven gas was nitrogen at a channel pressure of 21 psia*, the consequent shock Mach number (M_s) was 4.0 which is the tailored Mach number for this tunnel using helium : nitrogen operation. This gave a reflected shock pressure of around 2500 psi and a calculated temperature of 2000°K.

The object of the experiment was to deduce the aerodynamic static derivatives of the model by observing the convected motion of the model in the impulsive stream of the shock tunnel. The measured displacement of the model centroid with time permits the calculation of the aerodynamic force acting in the direction of the displacement. If the centroid and centre of aerodynamic pressure coincide, then the pitching moment is zero and the model maintains its incidence through the test section (Figs. 6, 7). When constant incidence is achieved, the motion of a specific point on each image can be scaled to real distance, both in a parallel and normal direction to the model main axis.

The centroid position of each model was deduced by a simple balancing jig, outside the tunnel, prior to hanging the model in the tunnel. The centroid was moved to the estimated centre of pressure, by internally adding a small bead of Araldite to the hollowed-out model. Centroid adjustment was continued until the measured incidence in flight remained within $\pm 0.5^\circ$ of the initial angle of incidence.

The time that each spark occurred was detected by a photodiode and recorded on a separate oscilloscope triggered from a common source upstream of the nozzle.

Since/

* 1 psi = 6895 N/M²

1 atm = 101325 N/M²

Since the movement of the model is proportional to the cross-sectional area but inversely proportional to the mass of the model, and the accuracy of reading from the photograph plate is proportional to the size of the model, a compromise was necessary from considerations of tunnel size. The maximum diameter of model that could be used was 1.46 in. (3.7 cm), making the total length of the model 7.15 in. (18.2 cm). A model movement of 2 in. in 8 ms required that this size of model should weigh less than 15 gm.

The flow was calibrated by separately flying three high-grade table-tennis balls of 1.50 in. (38 mm) diameter. The balls were suspended on a single thinned-thread. The drag coefficient of one of the spheres was assumed to be 0.915^4 at this test Mach number.

4. NPL Photographic Technique

The movement of HB-2 free-flight models was photographed with a multiple-spark light source² by making a series of discrete exposures on a single photographic plate. A sequence of partially superimposed images, suitably spaced in time, gave a convenient method for the measurement of the body movement.

A conventional single-pass Schlieren system was used with the normal knife-edge or graded filter removed, thus giving the equivalent of a focussed direct-shadow at the camera position. It was found that there was a limit to the number of images that could be exposed on one photographic plate (about ten) before it became difficult to distinguish each individual image. In order to maintain sufficient contrast, no more than 7 images were exposed on any one plate. By suitably selecting the time interval (typically 1 ms) between each successive spark, 4 or 5 images were obtained during the level-pressure time - representing the usable running time of the tunnel. Special photographic plates suited to a sequence of micro-second spark light flashes were supplied by Ilford Ltd. They are designated Fast Blue Sensitive Type L.N. plates made to order under experimental laboratory conditions. The plates were developed in Ilford 1D-19 which is an active MQ developer recommended for use when high contrast results are required from normal development and fixing solutions.

5. Calculation of Aerodynamic Forces

The reservoir pressure and test-section pitot pressure are step-like in character (Fig. 3) and have a steady pressure duration of about 6 ms. Pneumatic and electrical low pass filters have degraded the rise time of the signals in Fig. 3, the actual rise being faster than indicated. Because there is a finite time for flow establishment about the model, it is not possible to state at what instant of time the model began to move under the action of the applied force. The trajectory cannot, therefore, be deduced from the apparent initial conditions. However, by assuming a trajectory of the form $x = at^2 + bt + c$, where 'x' is the displacement at a given time 't', and fitting all the values of x and t (obtained from the photograph), by means of a least-squares criterion, the best possible linking equation is obtained from the experimental data.

Initially,/

Initially, solutions of the parabolic equation were obtained by direct substitution of pairs of values of x,t or y,t but this demonstrated that errors existed in displacement and time measurement which grossly affected the determination of the parabola coefficients, and therefore gave rise to proportional errors in the estimation of the force coefficients.

Typical values of $x^{\frac{1}{2}},t$ are plotted in Fig. 8 and show an excellent straight-line dependence. However this graphical presentation gives only a qualitative guide to the value of the force coefficients, and the least-squares approach is to be preferred for obtaining greater accuracy. In fact the least-squares fit resulted in a considerable improvement in run-to-run repeatability and in the value of the deduced coefficient. The coefficient 'a' is proportional to the force coefficient, 'b' and 'c' define hypothetical initial conditions of velocity and displacement respectively, that the model would have had if the quasi-steady state flow conditions had been established immediately.

The HB-2 results were correlated by a free-flight sphere test and an assumed drag coefficient. The repeatability of the drag coefficient of three successive sphere shots was within $\pm 1.5\%$. One of these (Run 1350) was used as the reference, and model weights and tunnel reservoir pressures were used in the normalising of the data. This meant that it was not necessary to define the nozzle Mach number when evaluating the results.

The correlation was carried out as follows:-

Since C_{A_t} is proportional to $w.a/P.S$

where w = weight of free-flight model

C_{A_t} = total axial-force coefficient

P = equivalent reservoir pressure as defined by Wilson and Regan⁵

S = a reference cross-sectional area of the model

a = coefficient of t^2 in the best-fit parabolic equation

then if C_{A_t} for the sphere is C^* , C_A for any other model

becomes $C_{A_t} = k \frac{wa}{PS} \cdot C^*$

where k is value of $\frac{PS_1}{wa}$ for the sphere run being used for

comparison, S_1 is the sphere cross-section, and C^* is the value of drag coefficient for a sphere at these velocities, and is taken as 0.915. The value of P is very close to the value of the measured reflected shock pressure, but is corrected to allow for real gas nozzle flows.

The/

The normal-force coefficient C_N was deduced in a similar way to C_A by fitting values of y and t to a different parabola.

Since C_A and C_N are directly proportional to x and y , the ratio $\frac{C_N}{C_A}$ (i.e., $\frac{N}{A}$) is the tangent of the angle of projection of the model, (e.g., if $C_N = C_A$, then the motion is at 45° to the initial attitude of the model).

Measurements of the pitching-moment coefficient C_m elsewhere adopted a reference-moment centre at a distance $1.95d$ from the nose of the model. The distance of the actual centre of pressure from this reference was non-dimensionalised by the body-diameter d , and the pitching-moment coefficient obtained by multiplying by the normal-force coefficient.

6. Discussion of Results

It was most encouraging to find that the three sphere runs gave comparative drag coefficients within $\pm 1.5\%$. The standard deviation of the coefficient of t^2 in the parabolic equation was about 1% for all three runs, demonstrating that the acceleration and hence the imposed force was uniform. With the HB-2 the repeatability from run to run of axial-force coefficient amounted to $\pm 2\%$ and of normal-force coefficient $\pm 9\%$.

The values of C_{A_t} , C_N , C_m obtained are compared in Figs. 9a, 9b and 9d, with the AEDC, BRL and DVL data, measured with force balances. The following tunnel conditions were employed:-

	AEDC ⁶	DVL ⁷	BRL ⁸	NPL
M_∞	8.09	8.75	9.16	8.6
Re_d	21×10^5	9×10^5	3×10^5	1.83×10^5
$d(\text{in.})$	7.50	1.18	2.00	1.46

6.1 The flow establishment about the model

From considerations of nozzle starting time and the rapid acceleration of the model into the stream, it might be pessimistically thought that the flow field around a sting-mounted HB-2 might be different from that about a freely-flying HB-2. In Fig. 4 the two conditions are compared and found to be identical. The bow shock and the angle of separation due to the flare are measured to be identical.

6.2 Total axial-force coefficient

The NPL and DVL total axial-force coefficient data are compared with AEDC forebody axial-force coefficients together with base-force coefficients estimated from base-pressure measurements. Fig. 9 shows good agreement with the DVL data in the range $0 \leq \alpha \leq 12^\circ$, both sets of data being some 11% higher than AEDC at $\alpha = 12^\circ$.

Fig. 5 shows that at $\alpha = 0^\circ$ there is no lifting force acting on the model. The contrast is arranged so that the five images can be seen. The reading accuracy can be improved by enlarging a portion of the photograph.

6.3 Normal-force coefficient

The amount of scatter in the NPL data (Fig. 9b) is disappointing at $\alpha = 6^\circ$; however at $\alpha = 12^\circ$ it amounts to only $\pm 7\%$, and the overall trend is in reasonable agreement with results from AEDC, DVL and BRL. The fact that $C_N = 0$ at $\alpha = 0^\circ$ (Fig. 5) shows that the shock tunnel nozzle flow is symmetric.

6.4 Ratio of normal force to axial force

Included in Fig. 9c are the values of N/A_t obtained from measuring the model's angle of motion relative to its initial attitude. The angle cannot be directly measured to better than $\pm 0.25^\circ$.

6.5 Pitching-moment coefficient

The NPL free-flight measurements (Fig. 9d) are consistently lower than AEDC data. At $\alpha = 12^\circ$ the values are about 30% less. Since the values of C_N obtained were in reasonable agreement, the difference must be due to the measurement of the centre of pressure. It is therefore interesting to see that the DVL measurements of C_m up to $\alpha = 10^\circ$ are consistently lower and at $\alpha = 10^\circ$ are only half the value obtained at AEDC. These low values of C_m may be due to a combination of three effects: (i) the estimation of centre of pressure, (ii) the difference in Mach number, and (iii) the range of Reynolds numbers of the separate data.

(i) It is not easy to define the centre of pressure position in free-flight measurements in short duration flows. When the centre of pressure position is destabilising, the model divergence is rapid and evident; but if the balance point (i.e., the centroid) is made to be stabilising, and is in fact ahead of the centre of pressure, the model may appear to be at constant incidence though in fact undergoing small stable oscillations which cannot be discerned in the short time of the test. In such a case the value of C_m would be underestimated. The constant incidence of the freely-flying models can be clearly seen in Figs. 6 and 7. The separation of the images is adequate for measurement; the sensitivity of the focussed direct shadowgraph is just sufficient for the bow shock waves to be discerned.

(ii)/

(ii) Comparison of the C_m data from AEDC, BRL and DVL at other Mach numbers shows that the value of C_m is strongly dependent on M_∞ , and is inversely proportional to M_∞ . At DVL, a change in M_∞ from 8.75 to 9.5 at the same Reynolds number reduces C_m from 0.2 to 0.07 at $\alpha = 10^\circ$; and at AEDC, for a change in M_∞ from 5.1 to 8.09 at constant Reynolds number, C_m reduces from 0.68 to 0.4 at $\alpha = 10^\circ$. It seems probable that the higher Mach numbers of NPL (8.6) and DVL (8.75) may partially account for the low values of C_m compared with AEDC (8.09), though this is not borne out by the $M = 9.2$ data of BRL which almost match the AEDC data.

(iii) Gray at AEDC notes that the pitching moment is sensitive to Reynolds number, though his presented data at $M_\infty = 8$ and $M_\infty = 10$ show very little dependence.

7. Conclusions

Measurements of axial-force, normal-force and pitching-moment coefficients on an HB-2 model have been made at the NPL by freely-flying models in a shock tunnel at $M_\infty = 8.6$.

The measurements were obtained by recording a sequence of images on to one photographic plate.

The results have been compared with force-balance data from the intermittent and continuous tunnels at the Arnold Engineering Development Centre, Tenn., U.S.A. and at the Ballistics Research Laboratories, Aberdeen Proving Ground, Maryland, U.S.A., and also with data from a gun tunnel at Deutsche Luft-und-Raumfahrt, Porz-Wahn, Germany.

Though values of C_N were in reasonable agreement with data from all centres, values of C_{A_t} from NPL and DVL were 11% higher than from AEDC, and values of C_m from NPL and DVL were at least 30% lower than from AEDC and BRL.

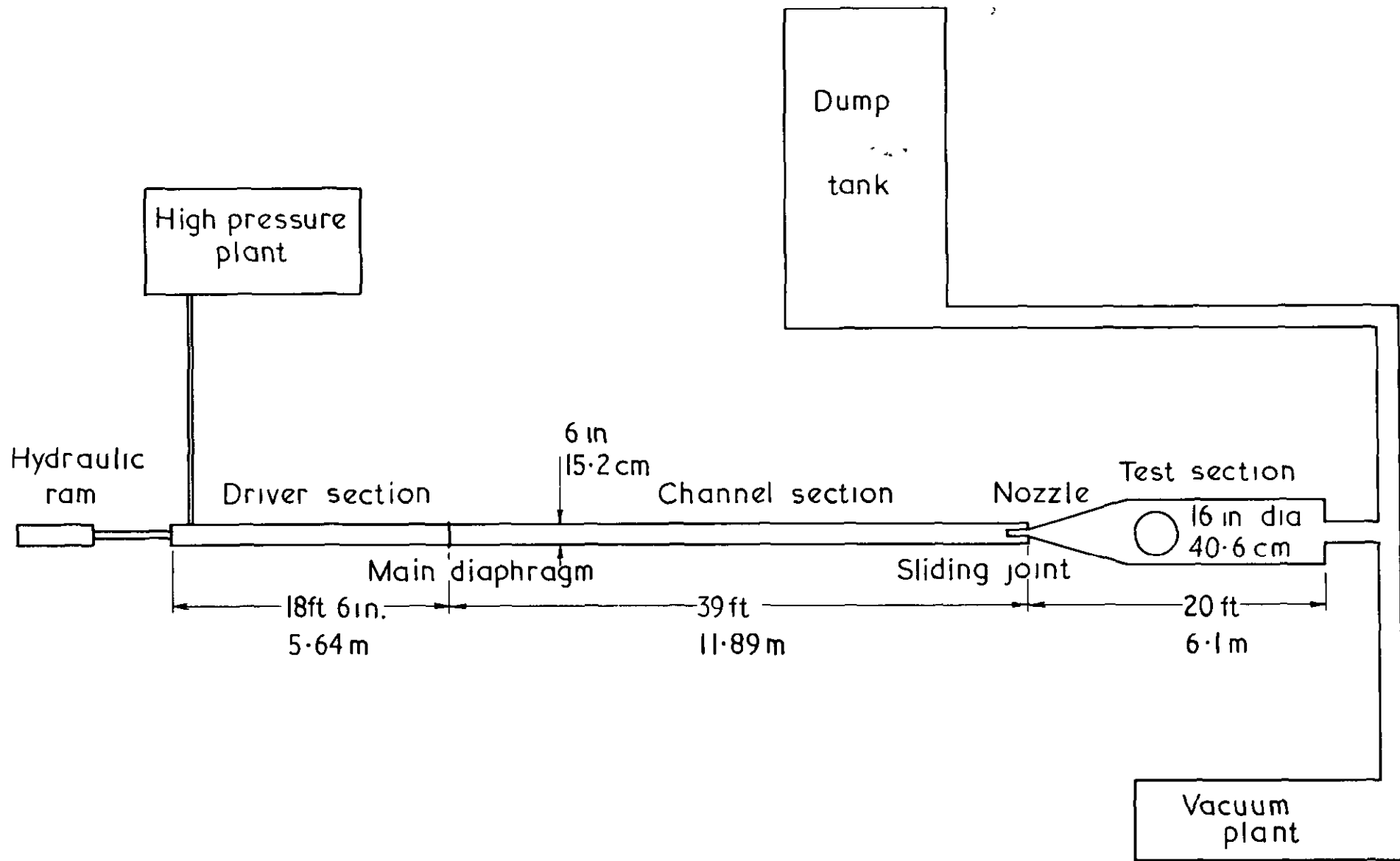
8. Acknowledgements

We are grateful

- (a) for the support of the Model Shop of the Division, under Mr. W. W. Smith, and in particular to Mr. David Simpson for making this series of foam plastic models,
- (b) for assistance by Dr. J. L. Wilson who suggested and provided the curve fitting programme, and
- (c) to Mr. A. Catley and Miss B. Redston who helped with the tunnel operation and data reduction.

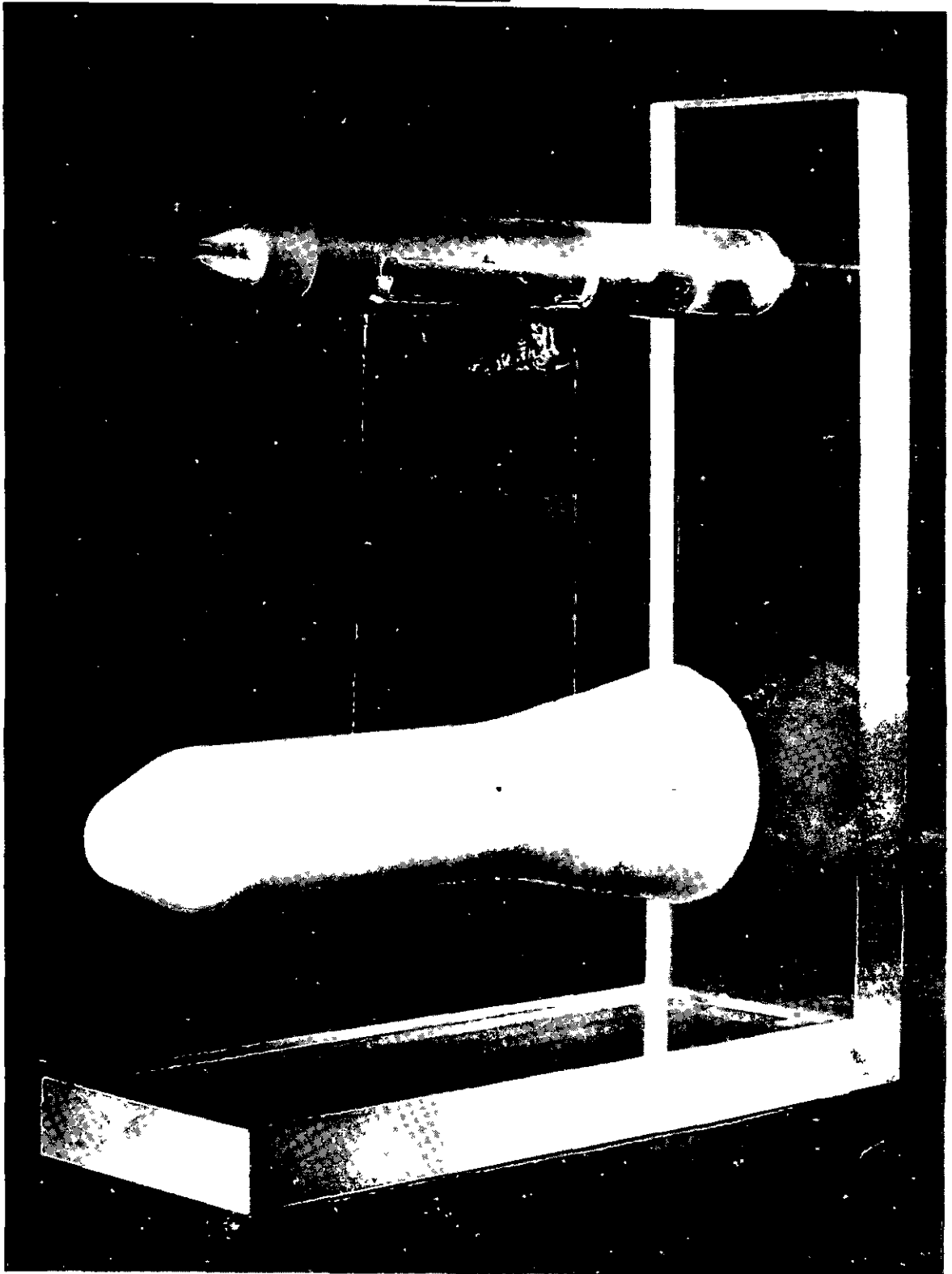
References

- | <u>No.</u> | <u>Author(s)</u> | <u>Title, etc.</u> |
|------------|--|---|
| 1 | R. E. Geiger | Experimental lift and drag of a series of glide configurations at Mach numbers 12.6 and 17.5.
Journal of Aerospace Sciences Vol.29, No.4, pp.410-419.
April, 1962. |
| 2 | R. F. Cash
and
M. J. Shilling | Schlieren photography of free-flight models in the NPL 6-in. shock tunnel using a high-speed framing camera or a repetitive spark light source.
NPL Aero Note 1031.
March, 1965. |
| 3 | L. Pennelegion,
R. F. Cash
and
D. F. Bedder | Design and operating features of the NPL 6-in. shock tunnel.
A.R.C. R. & M. 3449.
February, 1965. |
| 4 | A. J. Hodges | The drag coefficient of very high velocity spheres.
J. Aero. Sciences <u>24</u> , 10, pp.755-758.
October, 1957. |
| 5 | J. L. Wilson
and
J. D. Regan | A simple method for real gas flow calculations.
A.R.C. C.P.772.
February, 1964. |
| 6 | J. D. Gray
and
E. A. Lindsay | Force tests of standard hypervelocity ballistic models HB-1 and HB-2 at Mach 1.5 to 10.
AEDC-TDR-63-137.
August, 1963. |
| 7 | A. Heyser,
W. Wyborny
and
H.-P. Kabelitz | Dreikomponentenmessungen an den AGARD-Eichmodellen HB-1 und HB-2 im Stobwellenwindkanal mit freifliegendem Kolben.
DLR FB 66-25.
April, 1966. |
| 8 | K. O. Opalka | Force tests of the hypersonic ballistic standard models HB-1 and HB-2.
Unpublished work, private communication
Ballistic Research Laboratories, Aberdeen Proving Ground, Maryland, USA. |



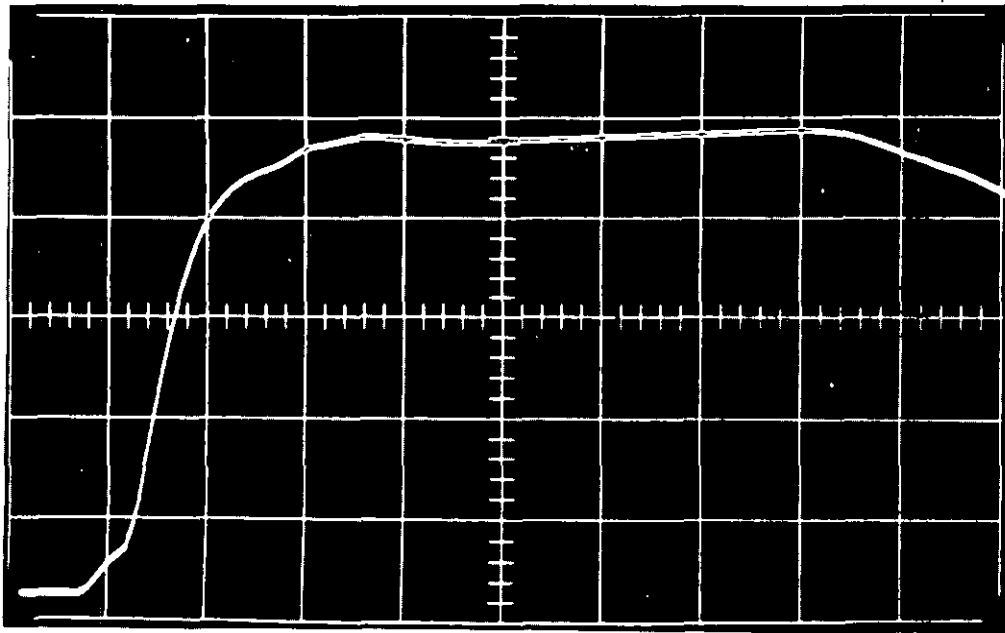
NPL 6 in (15.2 cm) Shock tunnel

FIG. 2



HB-2 Free flight suspension system

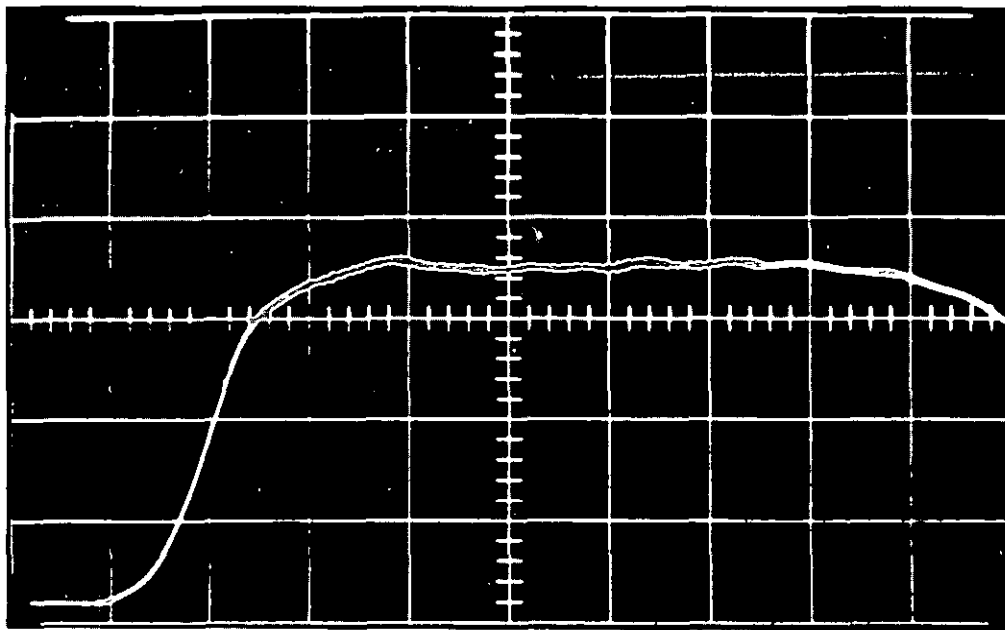
FIG 3



Reservoir pressure

→ 1mS ←

430 psia



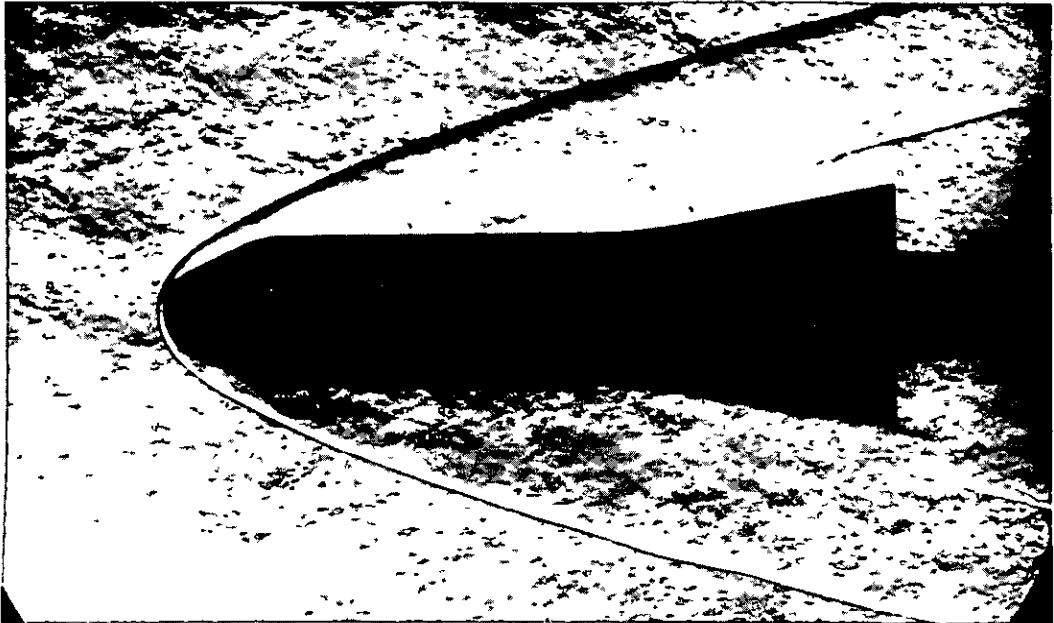
Pitot pressure

→ 1mS ←

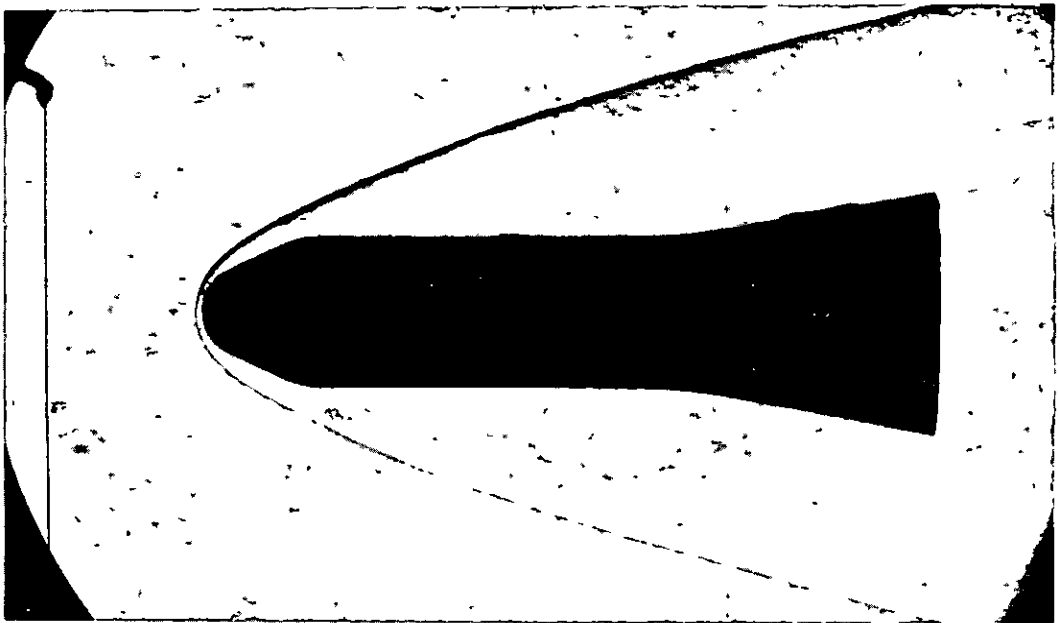
3.13 psia

Reservoir and pitot pressure records

FIG 4



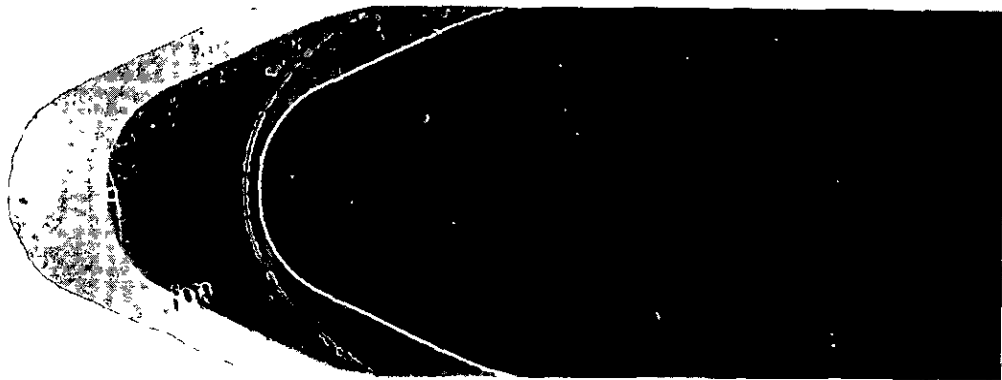
Sting mounted solid model



Single exposure of free flight model

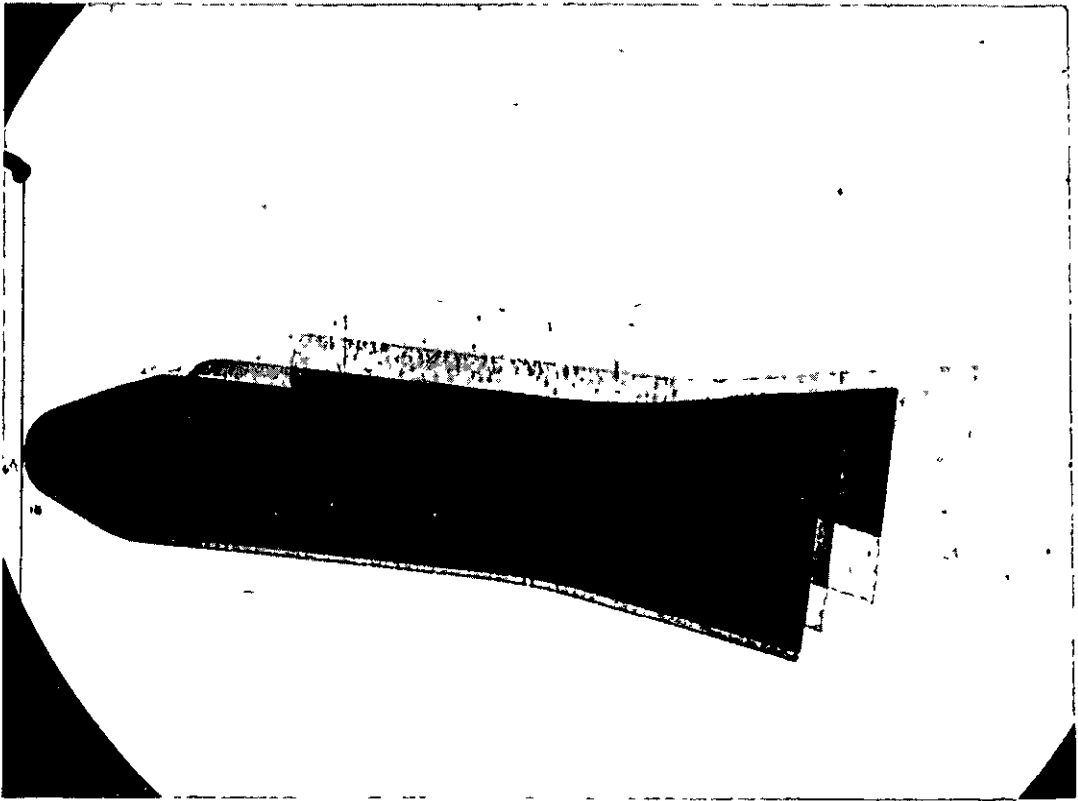
Comparison of free flight shock envelope with
static model envelope

FIG 5

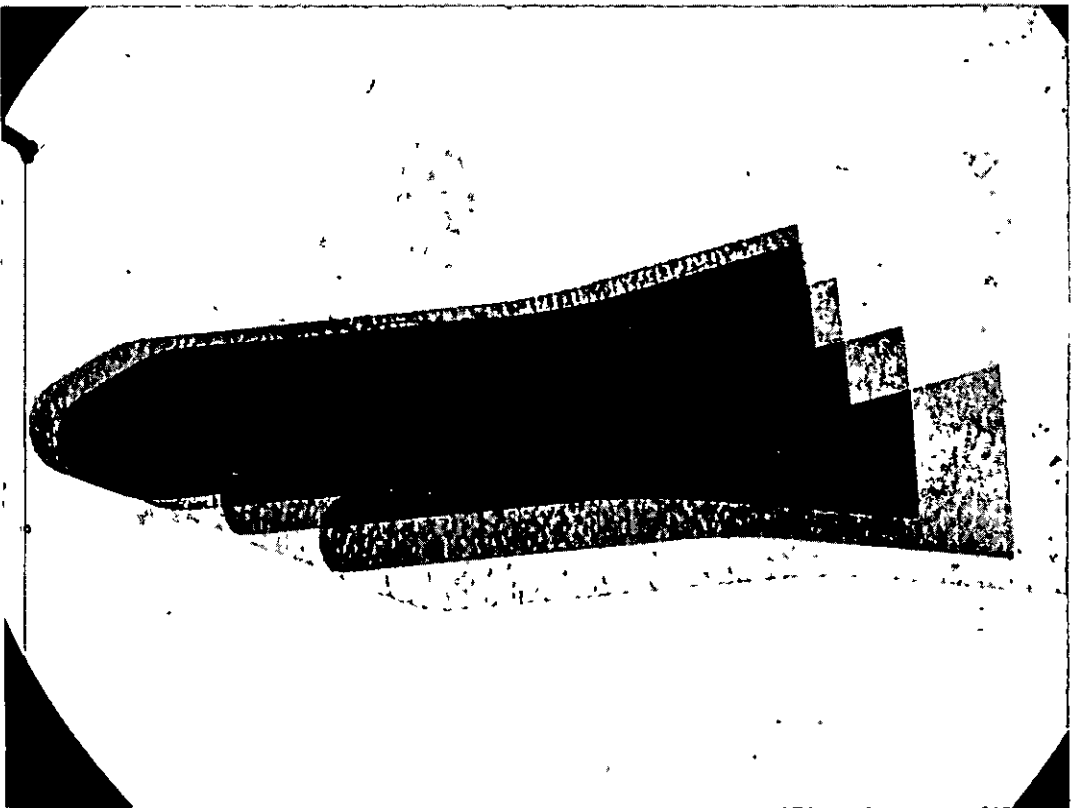


HB-2 Free flight, $\alpha=0^\circ$

FIG 6



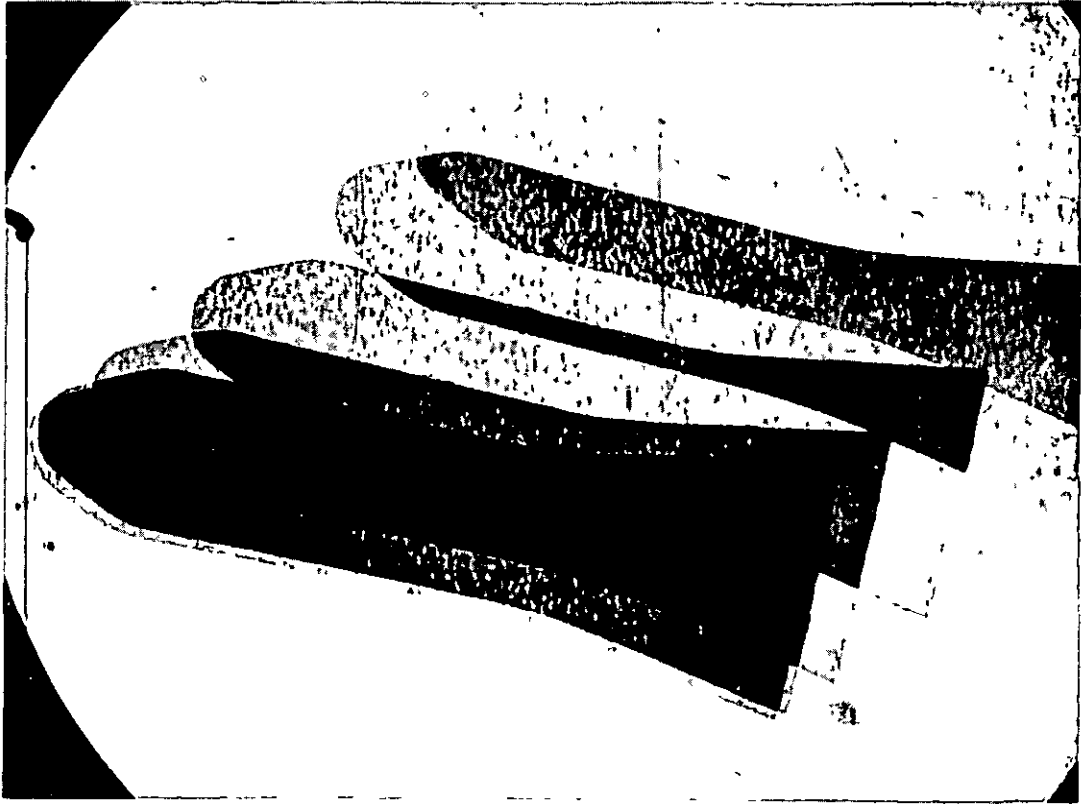
$\alpha = +6^\circ$



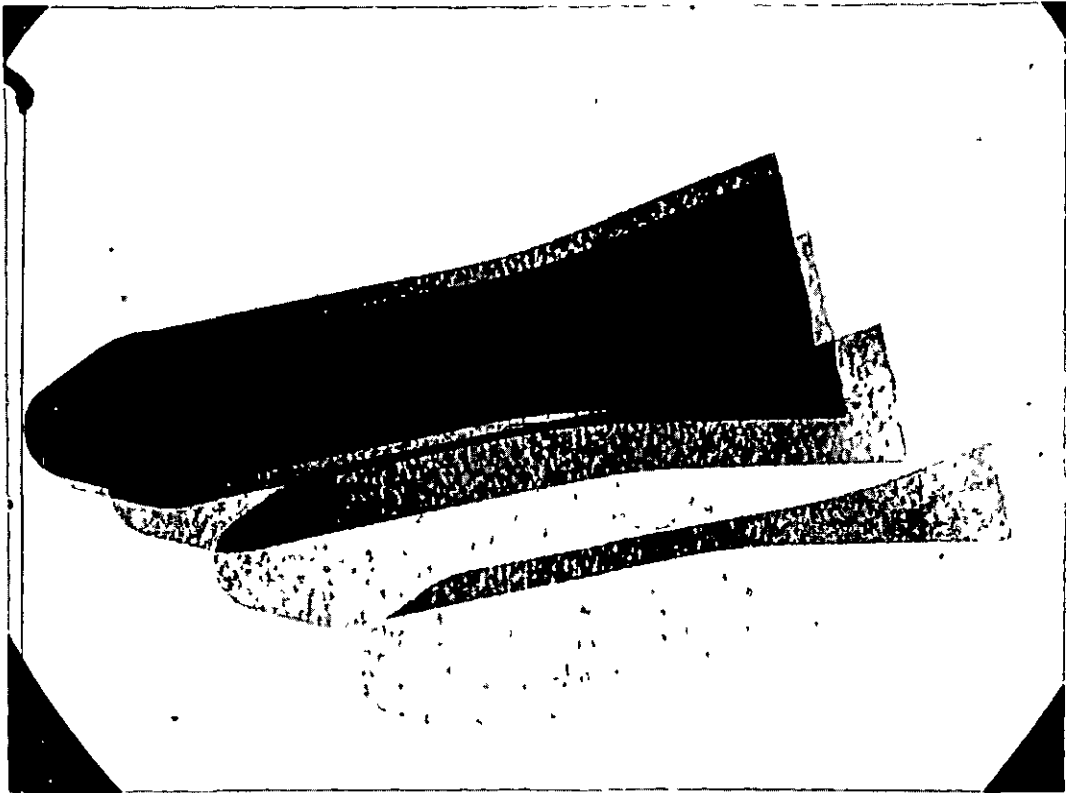
$\alpha = -6^\circ$

HB-2 Multiple spark photographs

FIG 7



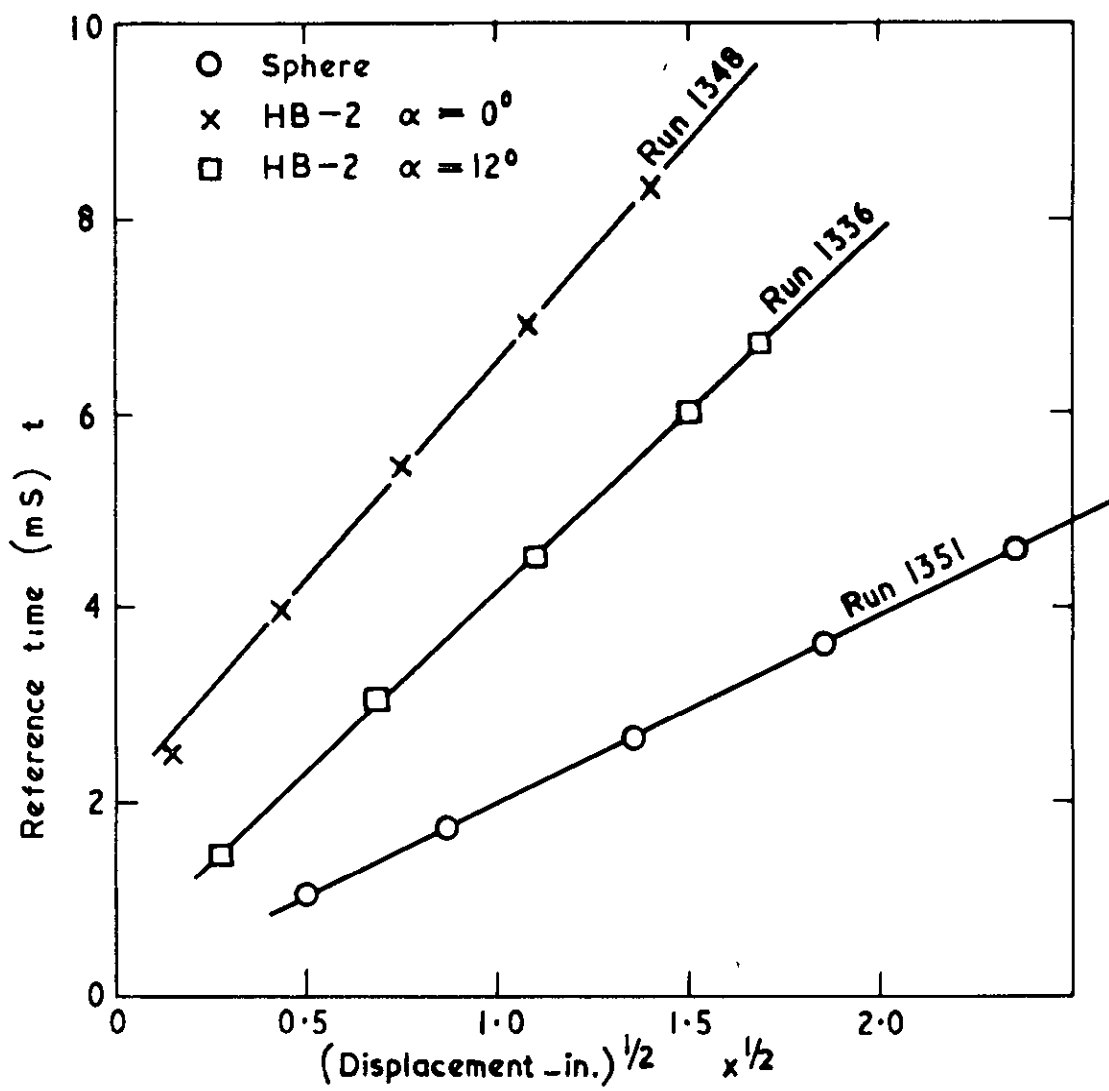
$$\alpha = +12^{\circ}$$



$$\alpha = -12^{\circ}$$

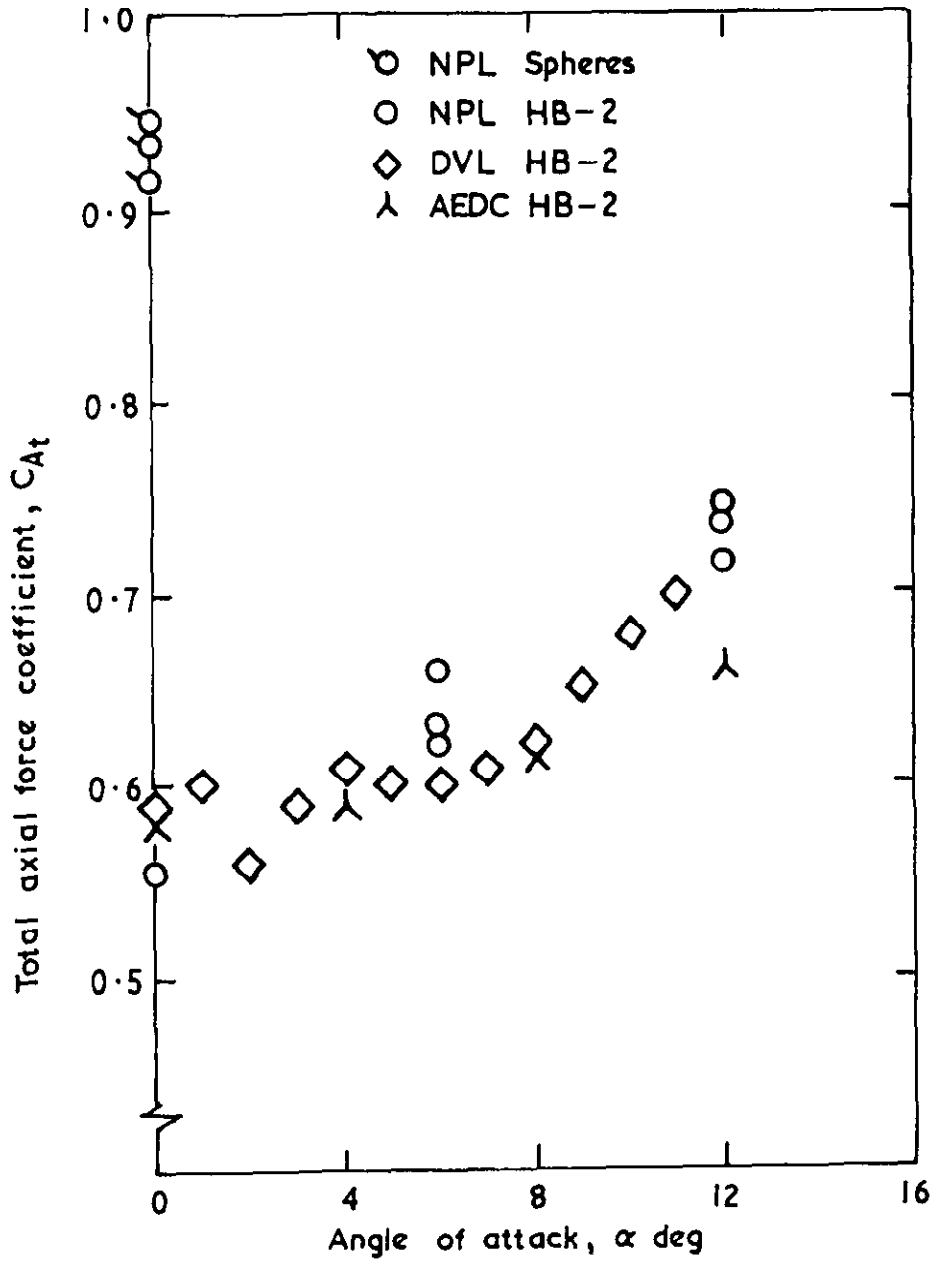
HB-2 Multiple spark photographs

FIG. 8



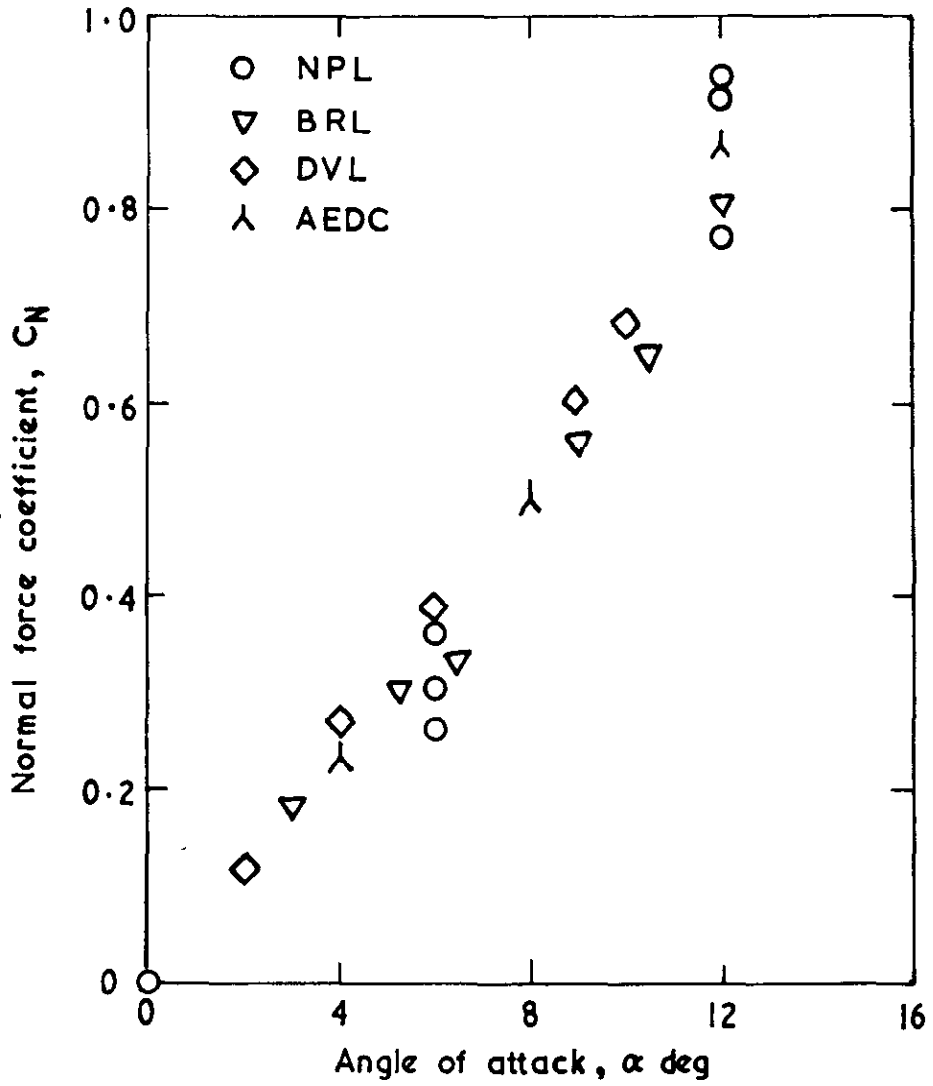
Axial movement of sphere and model HB-2

FIG. 9 a



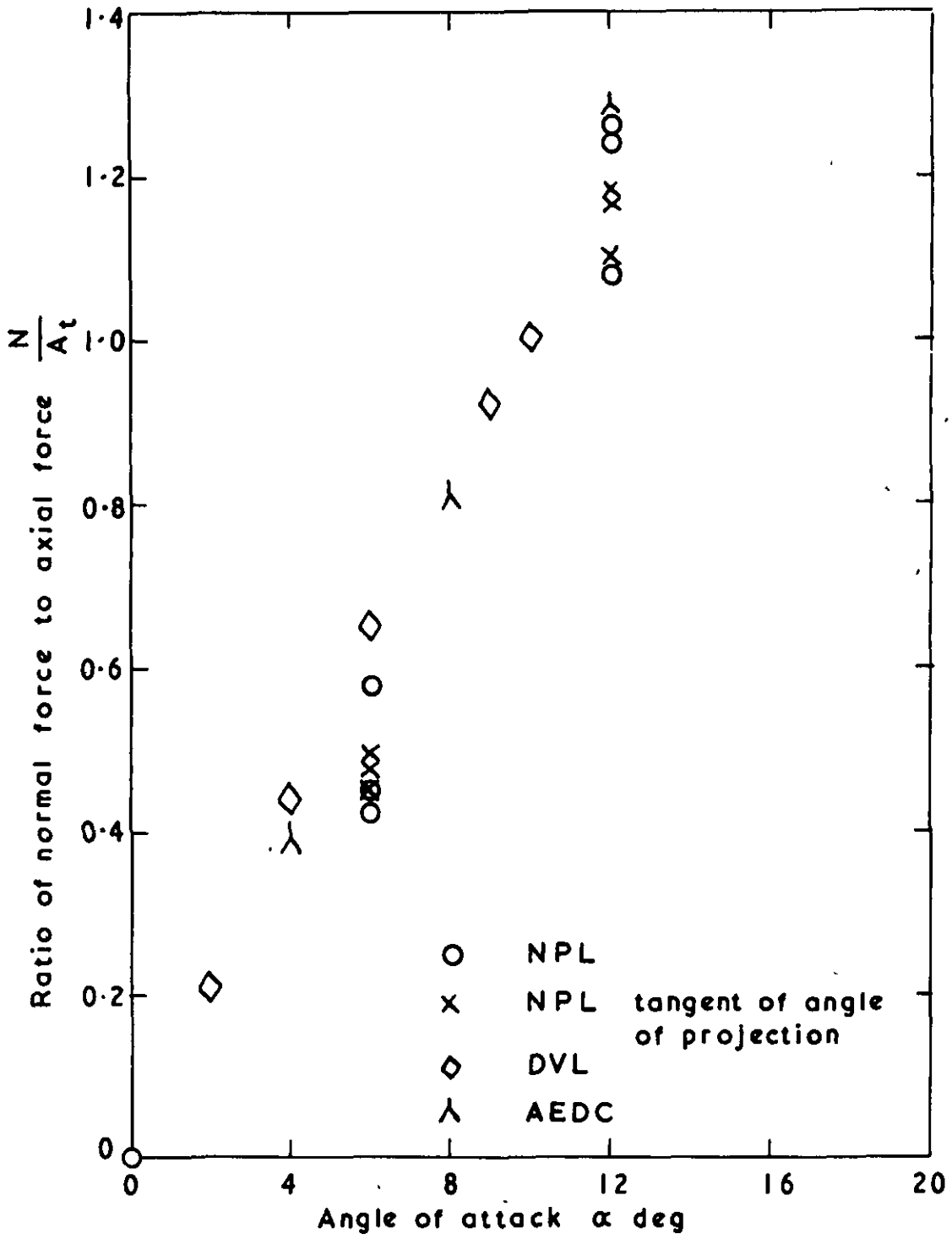
Total axial force for model HB-2

FIG. 9 b



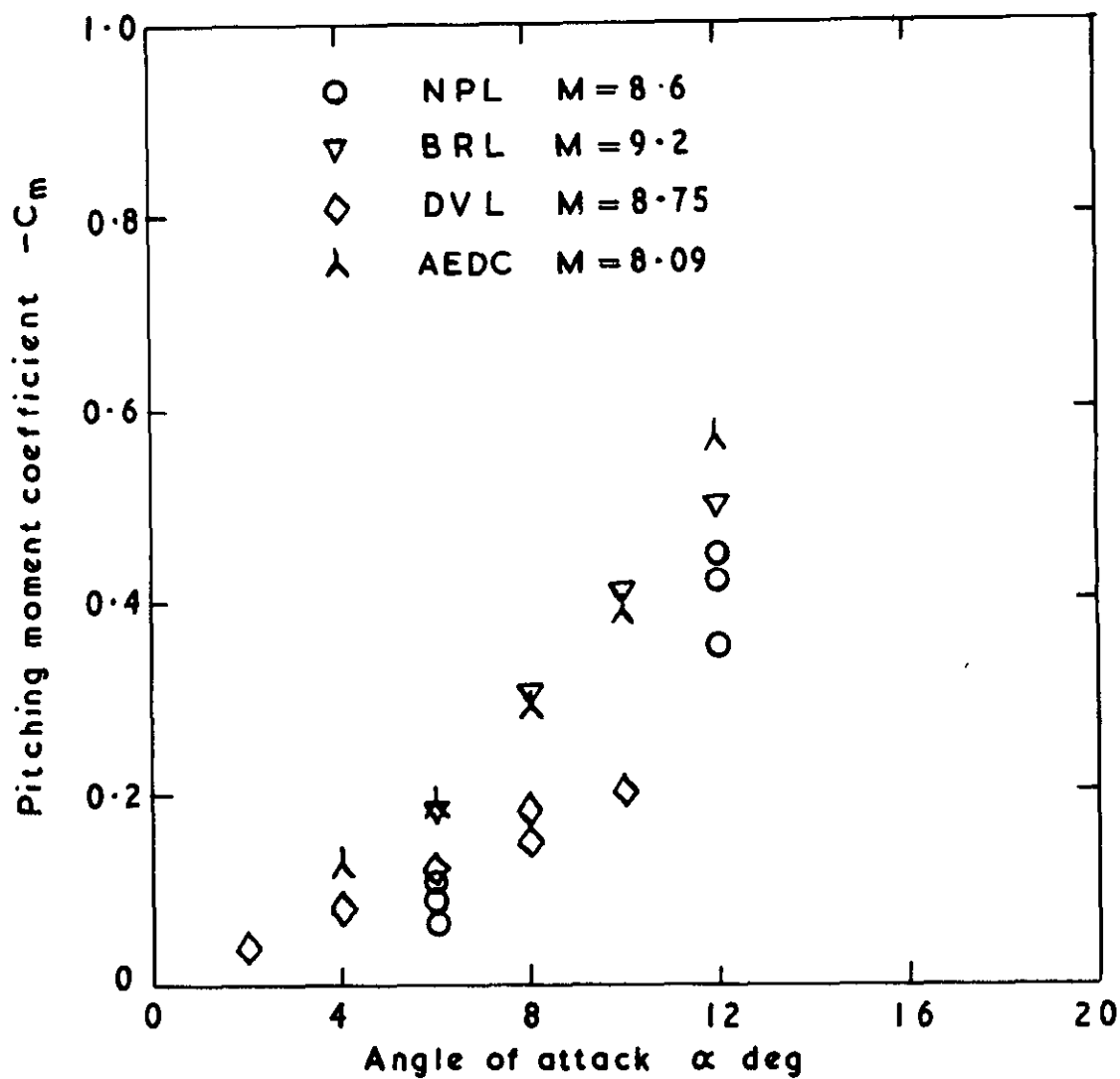
Normal force for model HB-2

FIG. 9 c



Ratio of normal force to axial force

FIG. 9d



Pitching moment for Model HB-2

A.R.C. C.P. No.934

October, 1966

L. Pennelegion, R. F. Cash and M. J. Shilling

FREE-FLIGHT TESTS IN THE NPL 6-IN. (15-CM) SHOCK
TUNNEL OF MODEL HB-2 USING MULTIPLE SPARK RECORDING

Free-flight measurements of axial force, normal force and pitching moment of an HB-2 model have been made in the NPL 6-in. (15-cm) shock tunnel and the results compared with force balance data obtained elsewhere. The displacement of the polyurethane models was recorded as a set of overlapping images on one photographic plate.

A.R.C. C.P. No.934

October, 1966

L. Pennelegion, R. F. Cash and M. J. Shilling

FREE-FLIGHT TESTS IN THE NPL 6-IN. (15-CM) SHOCK
TUNNEL OF MODEL HB-2 USING MULTIPLE SPARK RECORDING

Free-flight measurements of axial force, normal force and pitching moment of an HB-2 model have been made in the NPL 6-in. (15-cm) shock tunnel and the results compared with force balance data obtained elsewhere. The displacement of the polyurethane models was recorded as a set of overlapping images on one photographic plate.

A.R.C. C.P. No.934

October, 1966

L. Pennelegion, R. F. Cash and M. J. Shilling

FREE-FLIGHT TESTS IN THE NPL 6-IN. (15-CM) SHOCK
TUNNEL OF MODEL HB-2 USING MULTIPLE SPARK RECORDING

Free-flight measurements of axial force, normal force and pitching moment of an HB-2 model have been made in the NPL 6-in. (15-cm) shock tunnel and the results compared with force balance data obtained elsewhere. The displacement of the polyurethane models was recorded as a set of overlapping images on one photographic plate.

DETACHABLE ABSTRACT CARDS



© *Crown copyright 1967*

Printed and published by
HER MAJESTY'S STATIONERY OFFICE

To be purchased from
49 High Holborn, London w c 1
423 Oxford Street, London w 1
13A Castle Street, Edinburgh 2
109 St Mary Street, Cardiff
Brazennose Street, Manchester 2
50 Fairfax Street, Bristol 1
35 Smallbrook, Ringway, Birmingham 5
7 - 11 Linenhall Street, Belfast 2
or through any bookseller

Printed in England